RSC Advances

PAPER

View Article Online
View Journal | View Issue

Cite this: *RSC Adv.*, 2020, **10**, 20257

Approximately symmetric electrowetting on an oil-lubricated surface

Xi Yuan, [ab] Biao Tang, *[ab] Jitesh Barman, [ab] Jan Groenewold[abc] and Guofu Zhou[abd]

As the most widely used insulator materials in the electrowetting (EW) systems, amorphous fluoropolymers (AFs) provide excellent hydrophobicity, dielectric properties and chemical inertness; however, they suffer from charge trapping during electrowetting with water and the consequent asymmetric phenomenon. In this study, an ultra-thin oil-lubricated AF surface was proposed to release the charge trapping in the dielectric layer and further suppress the polarity-dependent asymmetry during electrowetting. The negative spontaneously trapped charges gathering on the dielectric/water interface with aging time were characterized by various measurements and calculations, which explained the polarity dependence of the asymmetric electrowetting. Approximately symmetric EW curves withstanding water aging were obtained for the oil-lubricated AF surface, confirming the blocking effect on charge trapping induced by the lubricated surface. The improved reversibility of EW with low contact angle hysteresis brought by the oil-lubricated surface was also demonstrated. This study reveals the mechanism behind the asymmetric EW phenomenon and offers an attractive oil-lubricated EW material system for suppressing the charge trapping on the dielectric/water interface, which can significantly improve the manipulation of the EW devices.

Received 15th March 2020
Accepted 9th May 2020

DOI: 10.1039/d0ra02405h

rsc.li/rsc-advances

Introduction

Electrowetting on dielectric (EWOD) offers a method to reversibly change the wettability of a droplet on an insulating substrate by applying an external voltage, enabling all kinds of applications, including lab-on-a-chip,[1–3] liquid lenses,[4–6] microfabrication,[7,8] energy harvesting,[9,10] heat transfer,[11,12] displays[13–15] and semiconductors.[16] Amorphous fluoropolymers (AFs) with good hydrophobicity,[17] dielectric properties (relative dielectric constant of ~2,[18] dielectric strength of ~200 V μm^{-1} (ref. 19)) and chemical inertness[20] are the most widely used materials in the EWOD system.[21–23] In EWOD devices, the variation in the contact angle with the applied voltage ideally follows the Young–Lippmann theoretical equation:[24]

$$\cos\theta_V = \cos\theta_Y + \frac{\varepsilon_0\varepsilon_r}{2d\gamma}U^2 \quad (1)$$

Here, θ_Y is the Young's contact angle, γ is the surface tension of the droplet, d and ε_r are the thickness and relative dielectric constant of the dielectric layer, respectively, ε_0 is the vacuum dielectric constant and U is the applied voltage.

Obviously, according to the Young–Lippmann equation, the electrowetting performance is only dependent on the magnitude rather than the polarity (positive or negative) of the applied voltage once other parameters are given. However, in practice, the extent of contact angle manipulation matching with theory and contact angle saturation show voltage polarity dependence during electrowetting.[19,25–28] The polarity dependence further contributes to asymmetric electrowetting. More and more evidence on the mechanism of such voltage-polarity-dependent asymmetric electrowetting points to charge trapping on the interface of the liquid and dielectric surface.[19,25,29] Verheijen *et al.* proposed a modified Young–Lippmann equation considering the trapped charges on the dielectric surface:[30]

$$\cos\theta_V = \cos\theta_Y + \frac{\varepsilon_0\varepsilon_r}{2d\gamma}(U - U_T)^2 \quad (2)$$

$$\sigma_T = \frac{\varepsilon_0\varepsilon_r U_T}{d} \quad (3)$$

Here, U_T is the voltage caused by trapped charges, and σ_T is the trapped charge density. The polarity and extent of the charges trapped on the interface under varied applied voltages can be calculated by fitting the experiment data with the modified Young–Lippmann equation. Wu Hao *et al.* demonstrated charge

[a]*Guangdong Provincial Key Laboratory of Optical Information Materials and Technology, Institute of Electronic Paper Displays South China Academy of Advanced Optoelectronics, South China Normal University, Guangzhou 510006, P. R. China. E-mail: tangbiao@scnu.edu.cn*

[b]*National Center for International Research on Green Optoelectronics, South China Normal University, Guangzhou 510006, P. R. China*

[c]*Van't Hoff Laboratory for Physical and Colloid Chemistry, Debye Research Institute, Utrecht University, Padualaan 8, 3584 CH Utrecht, The Netherlands*

[d]*Academy of Shenzhen Guohua Optoelectronics, Shenzhen 518110, P. R. China*

trapping during electrowetting *via* local contact angle measurements and quantitative characterization using Kelvin probe force microscopy.[31] Xie Na reported that the polarity of the driving voltage created significantly different responses of liquid lens since negative ions were more easily restrained in the dielectric layer.[32] Moreover, many researchers found that negative charges were likely to be spontaneously trapped at the fluoropolymer/water interface even without an external applied voltage.[33,34] Zimmermann *et al.* reported that the isoelectric point of AF was not related to the type of ions in solutions by zeta potential measurements, showing that the charge trapping on AF may be predominated by the particular adsorption of OH^-.[35] Banpurkar *et al.* further revealed that the spontaneously trapped charges aroused asymmetric electrowetting and the trapped charge density was related to the type and pH of the solution.[36] Many attempts on mitigating the charge trapping during electrowetting have been conducted. Balaji Raj *et al.* suggested that large-sized ions in testing liquids could reduce the charge trapping risk.[37] Xiangming Li *et al.* reported that the charge trapping-induced saturation could be suppressed by drive waveform modulation.[38] Some near symmetric electrowetting curves were found for an oil-lubricated surface, indicating improvement in charge trapping by introducing the oil layer.[30] However the hypothesis has not been validated yet. The trapped charges cause asymmetric responding,[29,31,36] saturation[30,38] and even dielectric failure[37,39] in EWOD devices, resulting in great challenges towards the reliability and precise manipulation of microfluidic devices. How to effectively reduce charge trapping is of great value for the development and applications of microfluidic devices.

In this paper, an ultra-thin oil layer-lubricated AF surface was introduced into the electrowetting system. The polarity and species of the spontaneous charge trapping on the AF/water interface with aging time were characterized by various measurements and calculations. The symmetry of the electrowetting performance on both original and oil-lubricated AF surfaces was systematically investigated.

Experimental

Fabrication of the oil-lubricated slippery surface

As shown in Fig. 1(a), Teflon AF 1600 (4.2 wt% in Fluorinert® FC43, Chemours) was deposited on detergent cleaned indium tin oxide (ITO) glass by spin-coating at 1000 rpm for 60 seconds, and a hydrophobic insulator layer with 1–1.5 μm thickness was obtained after a 85 °C thermally curing for 3 minutes and 185 °C annealing for 30 minutes. The perfluoropolyether (PFPE)-based oil (Krytox GPL 103, Dupont), which offers superior stability, lubricity, and great chemical compatibility with AF, was selected as the liquid lubricant. The Krytox oil was placed on the annealed AF surface with a fully wetted status (the contact angle was about 0°), followed by a dispersion process based on spin-coating at 1000 rpm for 60 s. After removing the excess oil gently, oil-lubricated slippery surfaces were obtained. The higher density of Krytox compared with water made the oil film stable under DI water.

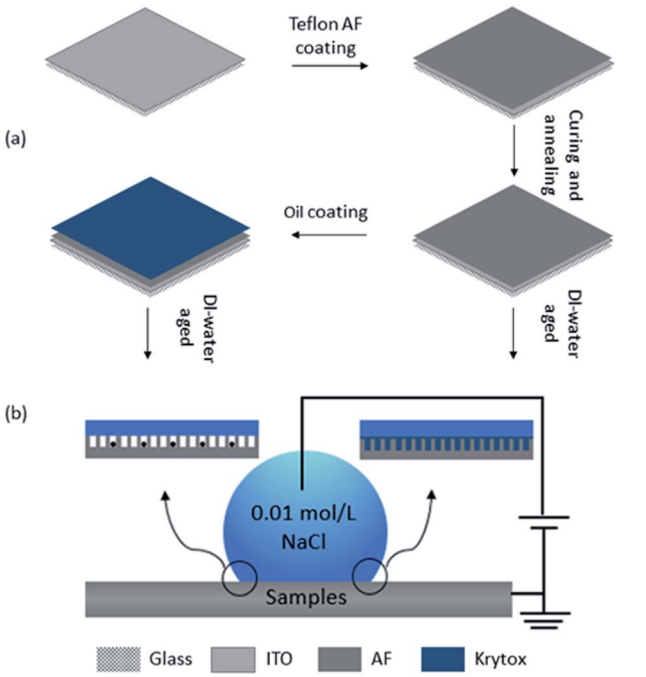

Fig. 1 Illustration of sample preparation and electrowetting tests. (a) The preparation of AF coating and oil-lubricated AF coating on ITO glass. (b) Electrowetting experimental setup. Insets depict the different interfaces of droplet-oil-lubricated AF surface (left) and droplet-AF surface (right).

Aging experiments and characterizations of trapped charges

The glass samples with the original AF surfaces and oil-lubricated AF surfaces were immersed into a beaker containing DI water. All the samples were horizontally placed in the water aging process. The samples were moved out and dried in a nitrogen atmosphere at a planned ending time for the subsequent characterizations and electrowetting experiments. The zeta potential measurements were taken at a constant pressure of 400 bar. A couple size of 2×1 cm^2 AF samples that had been aged for 24 hours were placed with a distance of 100 μm in the machine (Surpass, Anton Paar). The 0.001 M KCl solution was applied and its pH was automatically adjusted with HCl and NaOH. Zeta potentials were measured at varying pH.

The pH of initial water and that of water that has aged AF for 48 hours were measured. In order to exclude the pH changes caused by carbon dioxide dissolved in water, the pH of the water placed in air for 48 hours was also measured.

Electrowetting experiment

Fig. 1(b) shows the setup of the electrowetting conducted on samples. A 5 μL droplet of 0.01 mol L^{-1} NaCl solution was applied as one electrode in pair with the common electrode connected to ITO. A dc voltage from 0 V to 80 V was applied on the droplet and then, a dc voltage from 0 V to −80 V was applied on a new droplet. The step voltage 2 V s^{-1} was generated with a pico-ammeter (Keithley 6487). The contact angle changes with the applied voltage were recorded by using an optical contact angle goniometer (OCA 15). The electrowetting curves of the

NaCl droplet on the original AF surfaces in air and silicone oil (viscosity μ = 10 cSt, 1.1 gm cm^{-3}, Sigma-Aldrich) and on oil-lubricated AF surfaces in air were measured.

Results and discussion

The electrowetting curves for AF surfaces and oil-lubricated AF surfaces varying with the aging time in DI water are depicted in Fig. 2. For 0 hour AF samples, electrowetting experiments were directly performed on the freshly prepared samples. For 0 hour AF surfaces (both measured in air and silicone oil), the electrowetting curves were almost symmetric with the polarity of the applied voltage. However, for the AF surfaces that had been aging in DI water prior to the electrowetting experiments, the asymmetry of the electrowetting curves, especially for those measured in air, became more and more clearer on increasing the aging time, demonstrating that electrowetting was increasingly dependent on the polarity of the applied voltage. As for the curves measured in silicone oil, the symmetry changes were less obvious. Instead, it was noted that the oil-lubricated AF surfaces revealed striking symmetric electrowetting with the polarity of the applied voltage, which was not related to the aging time. In addition, the electrowetting response curves for the oil-lubricated AF surfaces after aging in DI water for 0 hour, 10 hours and 24 hours were basically unchanged. It seemed that both electrowetting in oil on AF and oil-lubricated layers on AF could improve the symmetry of electrowetting.

The presence of charges trapped on AF when the applied voltage was beyond the saturation voltage was proved.[30,31] The voltage applied in this work was smaller than the saturation voltage; thus, the effect of the trapped charges with the applied voltage is out of the scope of this work. It has been reported that the spontaneously trapped charges result in this asymmetric electrowetting behavior on AF.[25,36] Therefore, from the observation of almost symmetric and unchanged electrowetting curves on oil-lubricated AF surfaces, a hypothesis is proposed: this may be observed because the oil film stops AF from directly contacting with water, avoiding the accumulation of negative charges and then, the symmetric electrowetting performance is obtained. Based on eqn (2) and (3), the trapping voltage U_T and trapping charge density σ_T are extracted, as shown in Fig. 3. Minus U_T indicates trapped negative charges, and the absolute value of U_T means voltage caused by the trapped charges. Therefore, minus U_T on the AF surfaces (both measured in air and silicone oil) indicates that negative charges are trapped on AF during continuously contacting with DI water directly. The increasing absolute values of U_T and σ_T on AF surfaces indicate more and more charges being trapped with the prolonged aging time, resulting in the increase in asymmetric electrowetting. Instead, the values of both U_T and σ_T on the oil-lubricated AF surfaces are about 0, indicating little or no charge trapping on them; this further leads to symmetric electrowetting. The extracted U_T and σ_T on the AF surfaces measured in silicone oil are between the values of the AF surfaces measured in air and oil-lubricated AF surfaces; thus, we obtained less asymmetric electrowetting curves for the AF surfaces measured in silicone oil.

The details of the charge trapping mechanism on AF, especially the specific adsorption of ions, remain controversial. For further understanding, zeta potential and pH measurements

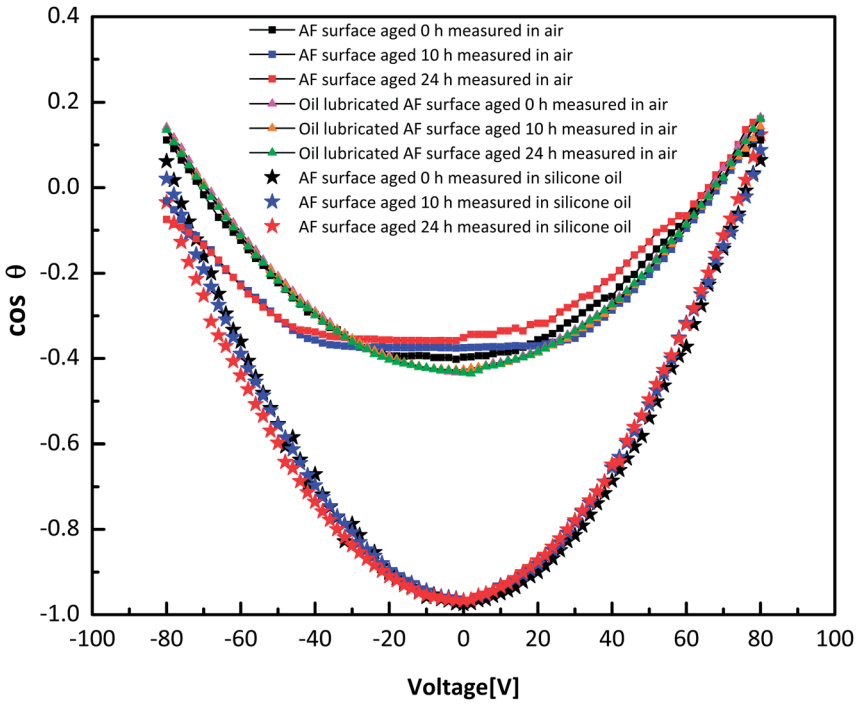

Fig. 2 Electrowetting curves on AF measured in air and silicon oil, oil-lubricated AF measured in air with aging in DI water for 0 hour, 10 hours and 24 hours.

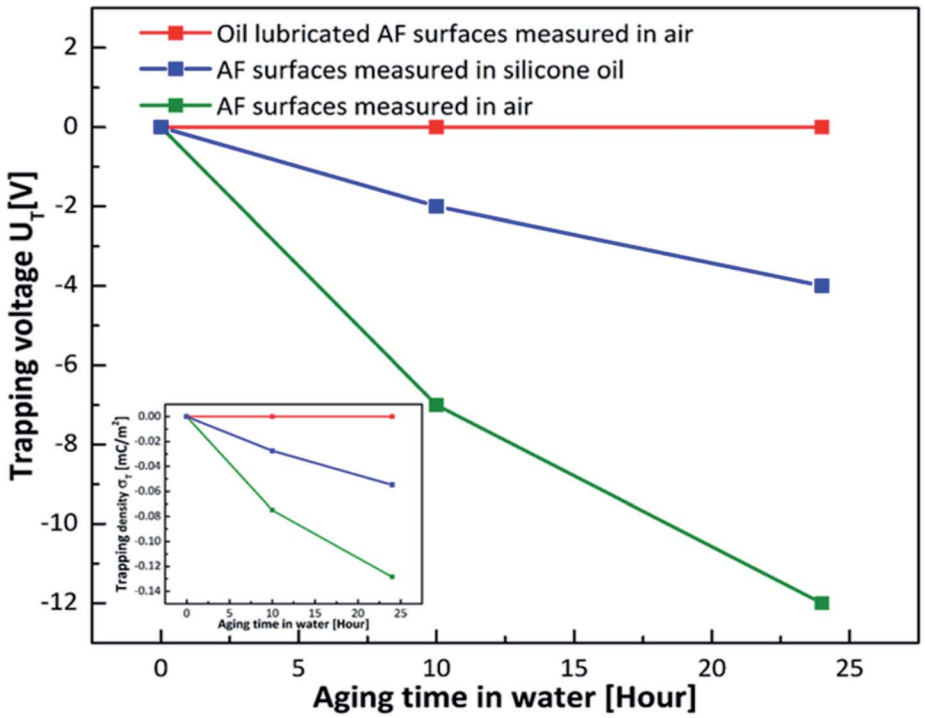

Fig. 3 The relationship between trapping voltage U_T and aging time. Inset: the relationship between trapping density σ_T and aging time.

were recorded. The zeta potential test can be used to measure the surface charge of a material. The zeta potential measurements on AF after aging for 24 hours in DI water are shown in Fig. 4(a). Consistent with references, the zeta potential became more negative on increasing pH and the isoelectric point of AF was about pH = 4.[35,36] It has been reported that water properties change at low dielectric hydrophobic surfaces, due to which hydroxide ions are preferentially adsorbed at the interface, resulting in negative surface charge and further negative zeta potential.[34] With the decrease in pH, protons neutralize this negative surface charge, leading to an isoelectric point at around pH = 4.[34] This result is consistent with the result of negative U_T. For ensuring the preferential adsorption of OH^-, the pH of the water used for aging AF surfaces for 0 hour and 48 hours was measured. In order to avoid the influence of HCO_3^- caused by the dissolution of CO_2 present in air in water, we also measured the pH of pure water before and after placing it in air for 48 hours; Fig. 4(b) reveals the results. It was obvious that the change in the pH of aging water was more severe than that of pure water. Because of the preferential adsorption of OH^- on the AF surface, the concentration of OH^- in the water used for aging the AF surface decreased, due to which the concentration

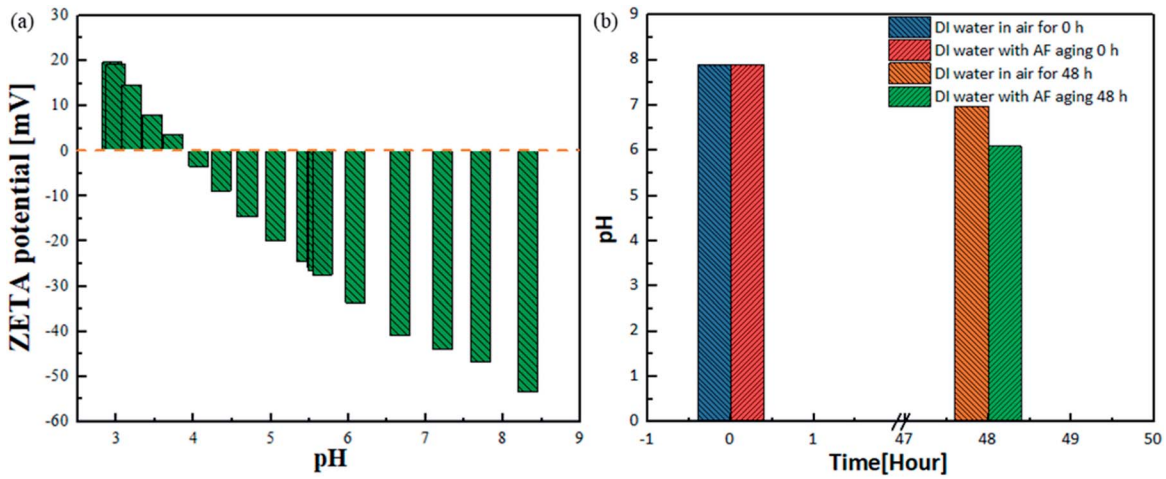

Fig. 4 (a) ZETA potential on AF surface after aging in DI water for 24 hours surrounding KCl solution with a concentration of 10^{-3} mol L^{-1}. (b) The pH of DI water in air and DI water with AF for 0 hour and 48 hours.

of H^+ increased relatively, resulting in pH reduction. This can provide evidence for the specific adsorption of hydroxide ions on the AF surface.

The comprehensive mechanism of symmetric electrowetting on oil-lubricated AF surfaces aged in DI water is still not entirely clear. Lubricating fluid-impregnated surfaces has drawn significant attention in electrowetting.[40–42] Low-voltage and

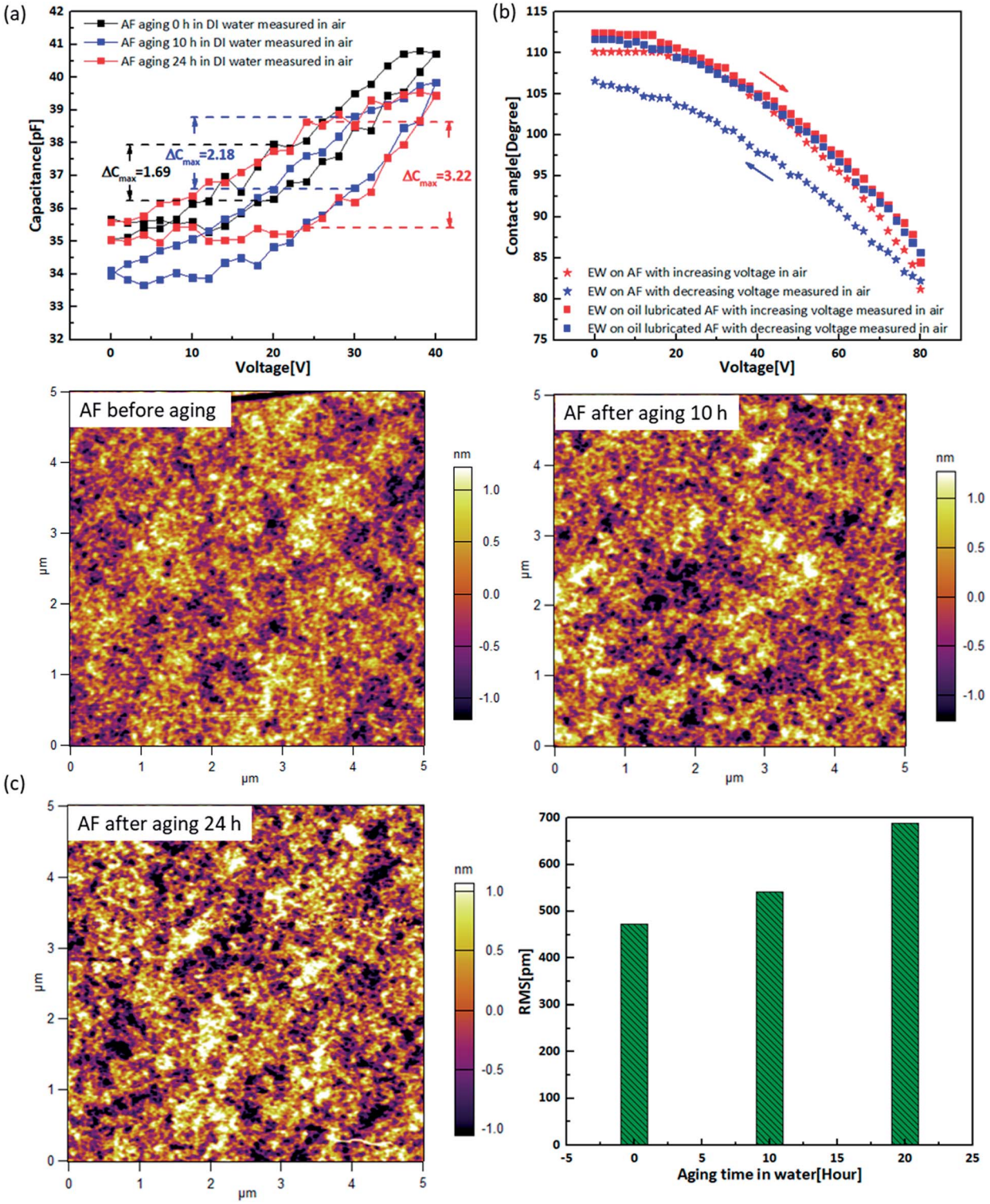

Fig. 5 (a) Capacitance *versus* voltage on AF surfaces aging in DI water for 0 hour, 10 hours and 24 hours. The maximum capacitance differences at the same voltage ΔC_{max} are marked. (b) Reversible electrowetting curves on AF surfaces and oil-lubricated AF surfaces all aging for 24 hours in DI water. (c) AFM images and roughness of AF before and after aging in DI water.

reversible electrowetting on oil-lubricated honeycomb polymer surfaces has been demonstrated[40] as the lubricant fluid conceals all chemical and topographical inhomogeneity[42] and offers a smooth motion for the three phase contact line of droplets.[41] In addition, the interfacial tension on the drop–lubricant interface is typically lower than that at the drop–air interface.[42] Therefore, lower contact angle hysteresis and low-voltage electrowetting have been reported on the lubricated surfaces. As we know, the internal composition of fluoropolymers is not dense enough, resulting in loose and porous structures. When the AF surface contacts with water directly, some small charged droplets or molecular species, for example, OH^- can move into the nanopores of the insulating layer and become trapped, which increase with the aging time in water, resulting in the increase in the asymmetric electrowetting response on the surface. In contrast, when a fluorinated lubricant oil Krytox GPL 103 was present on the surface, oil molecules could penetrate into the surface holes; thus, the surface became extremely smooth and completely covered with Krytox GPL 103.[43] Then, the oil-lubricated AF substrate was immersed in DI water with the protection of oil; the negative charges could not move into the holes of AF and were trapped. Thus, symmetric electrowetting was obtained even though the sample had been aging in water for a long time.

The variation in capacitance with the applied voltage on the AF surfaces was also measured and depicted in Fig. 5(a), from which worse electrowetting reversibility with a longer aging time in DI water could be concluded. Contact angle hysteresis is related to the physical or chemical properties of the surface. In order to understand what happened to the AF surface during DI water aging, experiments using atomic force microscopy (AFM) were performed. Fig. 5(c) depicts the AFM images of the AF surfaces and surface roughness (RMS) with different aging times. The original AF surface was relatively flat, with an average RMS = 473.887 pm. After the surface was aged in DI water for 10 hours and 24 hours, it was studied using AFM again. Though the topography transformation was not so obvious, the surface roughness of AF increased with the aging time in DI water (RMS = 542.389 pm and 688.243 pm, corresponding to aging for 10 hours and 24 hours), resulting in an increase in contact angle hysteresis. Fig. 5(b) illustrates that the electrowetting hysteresis can be greatly reduced by the method of oil lubrication on AF even though the two samples have been aged in DI water for 24 hours. In this way, almost completely reversible electrowetting could be obtained. Combining the results inferred from Fig. 2 and 3, we can conclude that charge trapping occurs with the increase in AF's surface roughness; introducing oil can reduce or even restrain this phenomenon; and with the slippery nature of the oil-lubricated surface, electrowetting reversibility is improved.

Conclusion

Different symmetries of the electrowetting performance on AF and oil-lubricated AF with continuous aging in DI water could be observed. Systematic characterizations and analysis, including zeta potential measurements and electrowetting curve fitting, revealed that negative charges were trapped on the AF surface, leading to asymmetric electrowetting. According to the pH tests, we deduced that OH^- ions were trapped on the AF surface. Based on the electrowetting data with water aging and the calculations of trapping voltage, the introduction of an oil-lubricated layer blocked the charge trapping at the dielectric/water interface, leading to a significant improvement in the symmetry of the electrowetting curves with promising water-aging endurance. The slippery nature of the oil-lubricated surface enabled good electrowetting reversibility as well.

Conflicts of interest

There are no conflicts to declare.

Acknowledgements

We appreciate the financial support from the National Key R&D Program of China (No. 2016YFB0401505), Program for Chang Jiang Scholars and Innovative Research Teams in Universities (No. IRT_17R40), Science and Technology Program of Guangzhou (No. 201904020007, 2019050001), Guangdong Provincial Key Laboratory of Optical Information Materials and Technology (No. 2017B030301007), South China Normal University "Challenge Cup" Golden Seed Cultivation Project (No. 19HDKB02), MOE International Laboratory for Optical Information Technologies and the 111 Project.

References

1 V. Srinivasan, V. K. Pamula and R. B. Fair, *Lab Chip*, 2004, **4**, 310–315.
2 K. Ugsornrat, P. Pasakon, C. Karuwan, C. Sriprachuabwong, T. Maturos, T. Pogfay, A. Wisitsoraat and A. Tuantranont, *IEEE Sens. J.*, 2019, **19**, 8597–8604.
3 M. Torabinia, P. Asgari, U. S. Dakarapu, J. Jeon and H. Moon, *Lab Chip*, 2019, **19**, 3054–3064.
4 S. Yang, T. N. Krupenkin, P. Mach and E. A. Chandross, *Adv. Mater.*, 2003, **15**, 940–943.
5 B. Berge, Liquid lens technology: principle of electrowetting based lenses and applications to imaging, *International Conference on Micro Electro Mechanical Systems*, 2005, pp. 227–230.
6 X. Hu, S. Zhang, C. Qu, Q. Zhang, L. Lu, X. Ma, X. Zhang and Y. Deng, *Soft Matter*, 2011, **7**, 5941–5943.
7 J. Lee, H. Moon, J. Fowler, T. Schoellhammer and C. Kim, Electrowetting and electrowetting-on-dielectric for microscale liquid handling, *International Conference on Micro Electro Mechanical Systems*, 2002, vol. 95, pp. 259–268.
8 X. Li, H. Tian, Y. Ding, J. Shao and Y. Wei, *ACS Appl. Mater. Interfaces*, 2013, **5**, 9975–9982.
9 T. Krupenkin and J. A. Taylor, *Nat. Commun.*, 2011, **2**, 448.
10 T. Hsu, S. Manakasettharn, J. A. Taylor and T. Krupenkin, *Sci. Rep.*, 2015, **5**, 16537.
11 A. Sur, Y. Lu, C. Pascente, P. Ruchhoeft and D. Liu, *Int. J. Heat Mass Transfer*, 2018, **120**, 202–217.

12 K. Mohseni and E. S. Baird, *Nanoscale Microscale Thermophys. Eng.*, 2007, **11**, 99–108.
13 R. A. Hayes and B. J. Feenstra, *Nature*, 2003, **425**, 383–385.
14 H. You and A. J. Steckl, *Appl. Phys. Lett.*, 2010, **97**, 1–3.
15 R. Shamai, D. Andelman, B. Berge and R. Hayes, *Soft Matter*, 2008, **4**, 38–45.
16 S. Arscott, *RSC Adv.*, 2014, **4**, 29223–29238.
17 D. Liu and D. J. Broer, *Responsive Polymer Surfaces: Dynamics in Surface Topography*, John Wiley & Sons, 2017.
18 H. Liu, S. Dharmatilleke, D. K. Maurya and A. A. Tay, *Microsyst. Technol.*, 2010, **16**, 449.
19 E. Seyrat and R. A. Hayes, *J. Appl. Phys.*, 2001, **90**, 1383–1386.
20 F. Mugele and J. Heikenfeld, *Electrowetting: Fundamental Principles and Practical Applications*, John Wiley & Sons, 2018.
21 M. Paneru, C. Priest, J. Ralston and R. Sedev, *J. Adhes. Sci. Technol.*, 2012, **26**, 2047–2067.
22 S. Sohail, E. A. Mistri, A. Khan, S. Banerjee and K. Biswas, *Sens. Actuators, A*, 2016, **238**, 122–132.
23 Y. Deng, S. Li, D. Ye, H. Jiang, B. Tang and G. Zhou, *Micromachines*, 2020, **11**, 81.
24 F. Mugele and J.-C. Baret, *J. Phys.: Condens. Matter*, 2005, **17**, R705–R774.
25 A. Quinn, R. Sedev and J. Ralston, *J. Phys. Chem. B*, 2003, **107**, 1163–1169.
26 H. Moon, S. K. Cho, R. L. Garrell and C.-J. C. Kim, *J. Appl. Phys.*, 2002, **92**, 4080–4087.
27 S. Berry, J. Kedzierski and B. Abedian, *J. Colloid Interface Sci.*, 2006, **303**, 517–524.
28 B. Janocha, H. Bauser, C. Oehr, H. Brunner and W. Göpel, *Langmuir*, 2000, **16**, 3349–3354.
29 S. Berry, J. Kedzierski and B. Abedian, *Langmuir*, 2007, **23**, 12429–12435.
30 H. Verheijen and M. Prins, *Langmuir*, 1999, **15**, 6616–6620.
31 H. Wu, R. Dey, I. Siretanu, D. van den Ende, L. Shui, G. Zhou and F. Mugele, *Small*, 2020, **16**, 1905726.
32 X. Na, Z. Ning and X. Rong-Qing, *Jpn. J. Appl. Phys.*, 2018, **57**, 052201.
33 C. Tian and Y. Shen, *Proc. Natl. Acad. Sci. U. S. A.*, 2009, **106**, 15148–15153.
34 J. K. Beattie, *Lab Chip*, 2006, **6**, 1409–1411.
35 R. Zimmermann, N. Rein and C. Werner, *Phys. Chem. Chem. Phys.*, 2009, **11**, 4360–4364.
36 A. G. Banpurkar, Y. Sawane, S. M. Wadhai, C. Murade, I. Siretanu, D. van den Ende and F. Mugele, *Faraday Discuss.*, 2017, **199**, 29–47.
37 B. Raj, M. Dhindsa, N. R. Smith, R. Laughlin and J. Heikenfeld, *Langmuir*, 2009, **25**, 12387–12392.
38 X. Li, H. Tian, J. Shao, Y. Ding, X. Chen, L. Wang and B. Lu, *Adv. Funct. Mater.*, 2016, **26**, 2994–3002.
39 B. Dong, B. Tang, J. Groenewold, H. Li, R. Zhou, A. V. Henzen and G. Zhou, *R. Soc. Open Sci.*, 2018, **5**, 181121.
40 E. Bormashenko, R. Pogreb, Y. Bormashenko, H. Aharoni, E. Shulzinger, R. Grinev, D. Rozenman and Z. Rozenman, *RSC Adv.*, 2015, **5**, 32491–32496.
41 J. Barman, R. Pant, A. K. Nagarajan and K. Khare, *J. Adhes. Sci. Technol.*, 2017, **31**, 159–170.
42 F. Schellenberger, J. Xie, N. Encinas, A. Hardy, M. Klapper, P. Papadopoulos, H.-J. Butt and D. Vollmer, *Soft Matter*, 2015, **11**, 7617–7626.
43 X. He, W. Qiang, C. Du, Q. Shao, X. Zhang and Y. Deng, *J. Mater. Chem. A*, 2017, **5**, 19159–19167.